EXAMINING LUNAR SURFACE MATURITY AT A VARIETY OF WAVELENGTHS, FROM UV TO RADAR. A. M. Stickle[1], J. T. S. Cahill[1], J. A. Grier[2], B. Greenhagen[1], G. W. Patterson[1], [1]Johns Hopkins University Applied Physics Laboratory, Laurel, MD, 20723, USA (angela.stickle@jhuapl.edu),[2]Planetary Science Institute, Tuscon AZ USA.

Background: The physical evolution of the lunar surface with exposure to the space environment (particularly impacts) is termed "maturation", can take place over relatively short timescales, and has been attributed to the amount of glass and agglutinate content within the lunar soil [e.g., 1-8], the amount of trapped solar wind nitrogen [9], solar wind sputtering and vapor deposition [10-11], and/or the amount of sub-microscopic iron (SMFe) in the material. Studies show that the abundance of these glasses and agglutinates increases with age of the soil and can account for large portions of a given mature soil [e.g., 2,4,9,14]. Changes in physical properties of the lunar soil are quantified in terms of specific maturity indices (e.g., Optical maturity (OMAT) [13]), and thus soils are generally classified on the basis of one or more of these specific indices [3]. Though sampling maturity effects from different processes and on different time- and depth-scales, comparisons indicate that maturity of the soil can be tracked across wavelengths [14], which is a powerful tool when examining the surface evolution of the Moon.

Observations of Crater Age Across Wavelengths: There are a number of methods for representing maturity: e.g., OMAT, LROC, Diviner, Mini-RF. Using OMAT, [13] classify Byrgius A as "young", Dufay B as "intermediate" and Golitsyn J as "old". Here, we survey how these ages are manifested across wavelengths to examine if correlations exist for maturity indices as a function of wavelength.

Ultra Violet. UV data from LRO's LAMP and the LROC WAC provide the shortest wavelength view of maturity. Denevi et al. [15] examined the effects of space-weathering at ultraviolet wavelengths using seven-band color data from the LROC WAC, and suggest that UV reflectance data is a key diagnostic tool for quantifying maturation of the youngest lunar soils, especially locally. The WAC color data suggest that higher 321/415 nm ratio is expected for the most immature soils. A RGB image (e.g., Fig. 1 left) with R = 415 nm reflectance, G = 321/415 nm ratio, B = 321/360 nm ratio can be used to examine our three chosen craters. Green areas indicate the most mature soils, while reddish/pink areas indicate regions of low 321/415 nm ratio. Areas showing up yellow indicate high 321/415 nm ratio. Note that the ejecta for the youngest crater (Byrgius A, Fig. 1 top) possesses a high 321/415 nm signature, while the more weathered surfaces of the older craters progressively shift to the more mature background soils.

Diviner. Degradation of surface rocks can be observed using the rock abundance parameter derived from Diviner measurements [16]. A paucity of rocks indicates a more weathered, mature surface. This is also apparent in the nighttime surface temperature of the surface. Smaller particles retain heat less well and so will be colder at night than larger, coherent blocks and boulders, allowing this to be a proxy for weathering state of the surface. This is illustrated in Fig. 1, below (middle columns). With age, the rock abundance and nighttime temperatures decrease. Byrgius A has a high rock abundance in the ejecta blanket and comparatively warm nighttime soil temperatures than the older Dufay B and even older Golitsyn J. Analyses by [17] show that the Christiansen Feature (CF), a well-studied compositional indicator of silicate mineralogy, can also be used as an indicator of maturity [18-22]. The CF shifts to longer wavelengths with increasing maturity; given the similar surface compositions, it is expected that Byrgius A will have a CF at shorter wavelengths, while Golitsyn J will have the CF at the longest wavelength.

Mini-RF. The Circular Polarization Ratio (CPR) is commonly used in analyses of planetary radar data [23-24] and is given by: CPR = $(S_1-S_4)/(S_1+S_4)$. It is a representation of surface roughness on the order of the radar wavelength (e.g., meter scale features). Unweathered ejecta blankets will contain large, blocky material, which will scatter the radar signal and result in a high CPR. Byrgius A is a classic example of how a young crater shows up clearly in radar: the CPR is high in the continuous ejecta blanket and transitions slowly to lunar background levels through the discontinuous ejecta (Fig. 1, top). As craters age, the ejecta blanket will degrade, losing the rough signature (e.g., Dufay B and Golitsyn J, Fig. 1 middle and bottom).

The m-χ decomposition provides information about the scattering characteristics of the surface (i.e., how much of the power returned is polarized and what is its polarization state) [25-26]. $m = (S_2^2 + S_3^2 + S_4^2)^{1/2}/S_1$ and $\mathrm{Sin}(2\chi) = -S_4/mS_1$. These parameters are visualized in a color-coded image (e.g., Fig. 1, right; Fig. 2), with: R = $[m\ S_1\ (1 + \sin 2\chi)/2]$, G = $[S_1\ (1-m)]$, B = $[mS_1\ (1 - \sin 2\chi)/2]$, representing the amount of double bounced, volume scattered, and single bounced signal returning to the radar (respectively). As the radar wave interacts with the surface, it can be scattered off of various reflectors (e.g., single or double bounce), or through the surface (e.g., volume scattering). It is expected that

younger surfaces, with the presence of blocky material, will tend to scatter off of the larger rocks, resulting in higher double bounce signal returning to the radar while older material will experience higher levels of volume scattering as the radar wave passes through the regolith volume (Fig. 2).

Discussion: Comparisons indicate that maturity of the soil can be tracked across wavelengths. Further, more detailed comparisons are necessary to fully understand whether maturity trends, which are manifested differently at different wavelengths, can be correlated, which will provide a powerful tool when examining the surface evolution of the Moon, and determining relative ages between features.

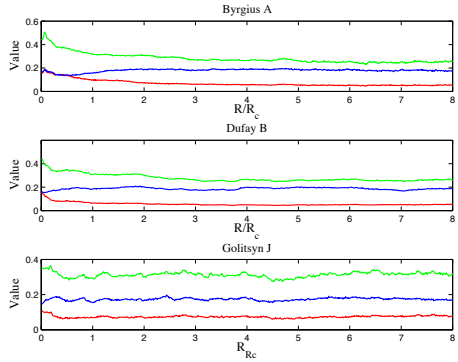

Figure 2. Mini-RF *m*-χ profiles for the three examined craters. As the craters age, structure is lost in the profile and a larger percentage of the material experiences volume scattering (shown in green, Golitsyn J, bottom) compared to double-bounce (shown in blue, Byrgius A, top). Dufay B is an intermediate case.

References: [1]Adams, J.B. and T.B. McCord (1971) *Science*, 171, 567-571; [2]McKay, D.S., et al. (1974) *Proc. Lunar. Sci Conf 5th,* p. 887-906; [3]Adams, J.B., and M.P. Charette (1975) *The Moon, 13*, 293-299; [4]Charette, M.P., et al. (1976) *Proc. Lunar Sci. Conf. 7th*, p. 2579-2592; [5]Wells, E., and B. Hapke (1977) *Science*, 195*,* 977-979*;* [6] Pieters, C. M. et al (1993) *J. Geophys. Res. Planet. 98*(E11), 20817-20824; [7] Britt, D.T., and C.M. Pieters (1994) *Geochim. Cosmochim. Acta 58*, 3905-3919; [8] Lucey, P. G., & Riner, M. A. (2011) *Icarus*, *212*(2), 451-462; [9] Charette, M.P., and J.B. Adams (1975), *Proc. Lunar Sci. Conf. 6th,* 2281-2289; [10] Gold, T., et al. (1976) *Proc. Lunar Sci. Conf. 7th*, p. 901-911; [11] Hapke, B., et al (1975) *Moon*, 13, 339-354; [12] McKay, D.S., et al. (1972) *Proc. Lunar Sci. Con;f. 3rd,* p. 983-994; [13] Grier *et al.* (2001) *J. Geophys. Res. 106*(E12)*,* 32847-32862; [14]Lucey, P.G., et al. (2000) *J. Geophys. Res., 105*, 20,377-20,386; [15]Denevi, B. et al. (2014) *J. Geophys. Res. Planet. 119,* 976-997; [16]Bandfield, J.L., et al. (2011) *J. Geophys. Res.*, 116, E00H02; [17] Greenhagen, B. T., et al. (2010) *Science*, 329, 1507-1509; [18] Conel, J. E.*, (1969), J. Geophys. Res., 74,* 1614–1634. [19] Greenhagen, B.T. (2009), *Ph. D. dissertation*, Univ. of Calif., Los Angeles, California, USA; [20] Lucey, P. G., et al. (2009) In *AGU Fall Meeting Abstracts* (Vol. 1, p. 0018); [21] Lucey, P. G., et al (2013), *Lunar and Planetary Science Conference*, XXXXIV, 2890; [22] Lawrence, D. J., et al (2014) *Icarus*; [23] Campbell et al. (2010), *Icarus*, 208, 565-573; [24] Carter et al. (2012), JGR, 117, E00H09; [25] Raney, R. K. et al. (2011), *Proc. of the IEEE*, 99, 808-823; [26]Carter et al. (2012), JGR, 117, E00H09.

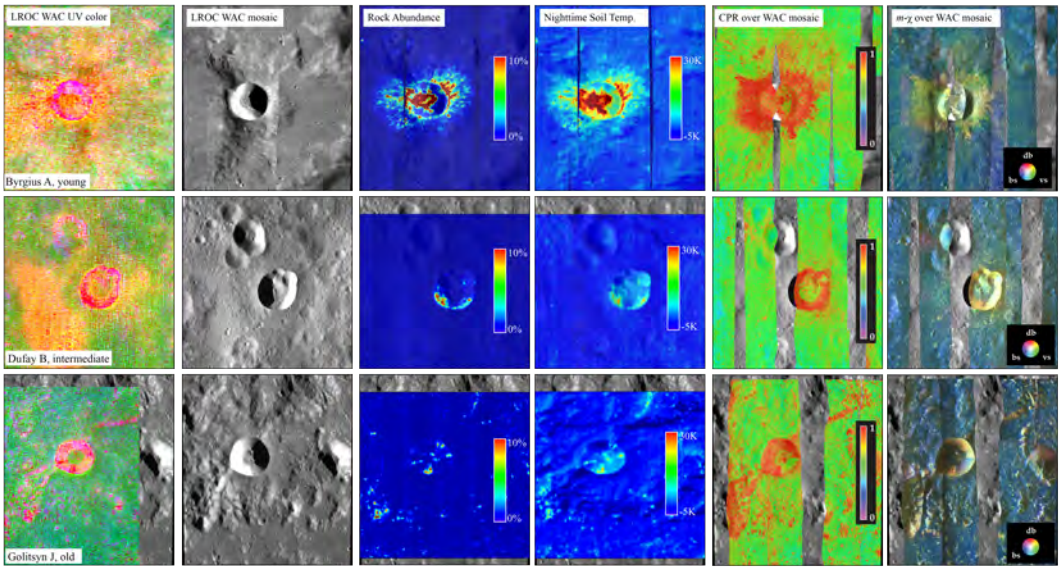

Figure 1. (top) Byrgius A (19.7 km, 24.6°S, 63.5°W), a young highlands crater, (middle) Dufay B (19.8 km, 8.3°N,171°E), an "intermediate" aged highlands crater, (bottom) Golitsyn J (19.5 km, 27.9°S, 102.9°W), an "old" highlands crater. The columns show the appearance of the crater across wavelengths, from UV (WAC UV, left) to radar (Mini-RF radar, right).